

Deconfinement and chiral aspects of the QCD crossover under magnetic fields: static-quark entropy and chiral susceptibility

Rishabh Thakkar,^{a,*} Heng-Tong Ding,^b Jin-Biao Gu^b and Sheng-Tai Li^b

^a*School of Science and Engineering*

The Chinese University of Hong Kong, Shenzhen, 518172, China

^b*Key Laboratory of Quark and Lepton Physics (MOE) and Institute of Particle Physics,
Central China Normal University, Wuhan 430079, China*

E-mail: rishabht@cuhk.edu.cn

We study the static-quark entropy in QCD under external magnetic fields and use the temperature at which it peaks – or equivalently, the inflection point of the renormalized static-quark free energy – as a pseudocritical deconfinement indicator. Calculations employ HISQ fermions with a tree-level improved Symanzik gauge action at physical quark masses, on lattices with $N_\tau=8,12$ and fixed aspect ratio $N_\sigma/N_\tau=4$. A two-dimensional (T, eB) analysis yields $S_Q(T, eB)$, from which we extract $T_{pc}^Q(eB)$ and obtain a continuum estimate. In the weak-field range explored, $T_{pc}^Q(eB)$ remains almost constant within uncertainties. We compare this deconfinement indicator with the peak of the total chiral susceptibility, finding compatible pseudocritical temperatures and a similarly weak eB dependence within current uncertainties. These continuum estimated results provide a controlled baseline for multi-observable studies of magnetic-field effects on the QCD crossover at physical quark masses.

*The 42nd International Symposium on Lattice Field Theory (LATTICE2025)
2-8 November 2025
Tata Institute of Fundamental Research, Mumbai, India*

*Speaker

1. Introduction

Understanding how strongly interacting matter responds to external magnetic fields is essential to describe QCD under extreme conditions. Strong magnetic fields may have influenced the evolution of the early Universe [1] and are present in astrophysical objects like neutron stars[2]. They are also present in heavy-ion collisions at RHIC and the LHC[3]. These fields can reach magnitudes comparable to intrinsic QCD scales, making it relevant to understand the response of the magnetic field to the QCD dynamics.

Considerable theoretical and lattice effort has clarified how magnetic fields affect chiral symmetry breaking and restoration [4–6]. Magnetic catalysis at low temperature and inverse magnetic catalysis near the crossover are now well established phenomena [7–13]. It is crucial to also explore the magnetic field response of the deconfinement aspect of the transition.

In QCD with physical quark masses at vanishing chemical potential, the transition is an analytic crossover. Different observables - chiral condensates, susceptibilities, Polyakov loop related quantities, and conserved charge fluctuations - need not yield identical pseudocritical temperatures. Recent studies indicate that the chiral crossover temperature shows minimal variation for $eB \lesssim 0.3 \text{ GeV}^2$ [8, 14], while conserved charge fluctuation χ_{11}^{BQ} , corresponding to the cross fluctuation between net baryon number and electric charge was singled out as a magnetometer, displaying significant magnetic sensitivity [14, 15]. This raises the question of whether deconfinement observables exhibit a different magnetic response from purely chiral ones. Thus, we address this question by examining the entropy of a static quark. The entropy peak provides an indicator of screening associated with deconfinement, corresponding to the inflection point of the renormalized static-quark free energy [16]. Using continuum estimated lattice results, we determine the magnetic field dependence of the associated pseudocritical temperature, while also providing the continuum estimated numerical values for thermodynamic observables such as entropy and free energy of a static quark in the medium.

2. Static-Quark Free Energy and Entropy

The Polyakov loop on the lattice is defined as

$$P(\mathbf{x}) = \frac{1}{3} \text{Tr} \prod_{x_0=0}^{N_\tau-1} U_0(\mathbf{x}, x_0), \quad (1)$$

where $U_0(\mathbf{x}, x_0)$ are the temporal link variables and N_τ is the number of points in the temporal direction on the lattice. The expectation value of the spatial average over volume V of $P(\mathbf{x})$ yields an estimate of the bare Polyakov loop

$$L^{\text{bare}}(B, T) = \left\langle \frac{1}{V} \sum_{\mathbf{x}} P(\mathbf{x}) \right\rangle. \quad (2)$$

The bare static-quark free energy is obtained from

$$F_Q^{\text{bare}}(B, T) = -T \ln L^{\text{bare}}(B, T) = T f_Q^{\text{bare}}(B, T), \quad (3)$$

where B is the external magnetic field strength, T is the temperature and the $f_Q^{\text{bare}}(B, T)$ is the dimensionless scaled bare static-quark free energy.

The bare Polyakov loop requires multiplicative renormalization to perform a continuum limit [17]. This multiplicative renormalization for the Polyakov loop results in an additive renormalization for the free energy. This renormalization constant can be fixed at $B = 0$ by exploiting the relation between the single static-quark free energy and the static quark-antiquark free energy [18],

$$\lim_{r \rightarrow \infty} F_{Q\bar{Q}}(r, B = 0, T) = 2F_Q(B = 0, T), \quad (4)$$

and matching $F_{Q\bar{Q}}(r, T)$ at short distances to the zero temperature static quark-antiquark potential [18].

In this work we employ the renormalization constant $c_Q(\beta)$ determined for the HISQ action in Ref. [16], where $\beta = 10/g_0^2$ denotes the bare lattice gauge coupling for HISQ action. The renormalized dimensionless free energy is then given by

$$f_Q^{\text{ren}}(B, T(\beta, N_\tau), N_\tau) = f_Q^{\text{bare}}(B, \beta, N_\tau) + N_\tau c_Q(\beta), \quad (5)$$

while the renormalized free energy reads

$$F_Q^{\text{ren}}(B, T(\beta, N_\tau), N_\tau) = T f_Q^{\text{bare}}(B, \beta, N_\tau) + C_Q(\beta), \quad (6)$$

where $C_Q(\beta) = c_Q(\beta)/a$ contains a divergence proportional to $1/a$ in the continuum limit canceling the divergence from the bare free energy. The renormalization constants are independent of the external magnetic field [19], since the ultraviolet self-energy of a static quark is insensitive to the external field.

The entropy of a static quark is defined thermodynamically as

$$S_Q(B, T) = -\frac{\partial F_Q^{\text{ren}}(B, T)}{\partial T} \quad (7)$$

$$= f_Q^{\text{bare}} + T \frac{\partial \beta}{\partial T} \frac{\partial f_Q^{\text{bare}}}{\partial \beta} + N_\tau \left(c_Q + T \frac{\partial \beta}{\partial T} \frac{\partial c_Q}{\partial \beta} \right). \quad (8)$$

Near the crossover region, the renormalized static-quark free energy exhibits an inflection point as a function of temperature. This inflection corresponds to a maximum in $S_Q(B, T)$ [20], reflecting the change in color screening properties of the medium. The position of this entropy peak therefore provides a crossover temperature T_{pc}^Q estimate for the deconfinement-like observable.

3. Lattice Setup

Simulations are performed in $N_f = 2 + 1$ QCD using the Highly Improved Staggered Quark (HISQ) action [21] and a tree-level Symanzik improved gauge action. The strange quark mass is tuned to its physical value by adjusting the mass of the fictitious strange quark pseudoscalar meson $\eta_{s\bar{s}}^0$ to $M_{\eta_{s\bar{s}}^0} = \sqrt{2M_K^2 - M_\pi^2} \simeq 684$ MeV [22], and light quarks are set by $m_l = m_s/27$, yielding $M_\pi \simeq 135$ MeV. The gauge configurations were generated using a modified version of the SIMULATeQCD codebase [23]. The lattice scale is set using the kaon decay constant f_K [24].

We use lattices with $N_\tau = 8$ and 12 and fixed aspect ratio $N_\sigma/N_\tau = 4$. Eight different β values span temperatures approximately $T \sim 140 - 175$ MeV. A constant magnetic field in the z direction is introduced via U(1) phases in the gauge links. The periodic boundary condition on a finite-volume lattice imposes flux quantization of the magnetic field [8]

$$eB = \frac{6\pi N_b}{N_\sigma^2 a^2} = 6\pi N_b T^2 \frac{N_\tau^2}{N_\sigma^2}. \quad (9)$$

The quantized magnetic flux quanta used here correspond to $N_b \in \{0, 1, 2, 3, 4, 6, 12\}$, yielding the magnetic fields in the range $eB \simeq 0 - 0.14 \text{ GeV}^2$.

4. Numerical Calculation

The Polyakov loop is computed on-the-fly during the generation of gauge configurations. The error was obtained using block bootstrapping with block size larger than autocorrelation length. The central value for the bare Polyakov loop expectation value is reported as the median of the corresponding bootstrap distribution, while its statistical error is defined using the 68.27% central quantiles.

4.1 Surface Interpolation and Statistical Uncertainties

Surfaces for the static quark free energy $F_Q(T, eB)$ and the entropy $S(T, eB) = -\partial F_Q/\partial T$ were obtained using a two-dimensional B-spline interpolation over the (β, eB) plane for the bare observable $f_Q^{\text{bare}}(\beta, eB)$. The `bisplrep` function of the `scipy.interpolate` package was used for the two-dimensional B-spline interpolation. The interpolation is performed independently for each available N_τ . The spline algorithm automatically determines the number and placement of knots based on the data error, subject to a tunable smoothing parameter s . The smoothing parameter is chosen such that it minimizes the variance of the residuals to prevent underfitting or overfitting. This corresponds to $s = 131$ and 65 for $N_\tau = 8$ and 12, respectively.

To estimate the statistical uncertainty, σ_{stat} , of the fitting procedure, we use the bootstrap resampling method. The statistical error is defined as the 68.27% central quantile of the bootstrap distribution. The systematic uncertainty from the fit ansatz is evaluated by varying the polynomial orders of the spline interpolation. The central result is obtained using polynomial orders $(\beta, eB) = (3, 3)$. To assess the stability of the fit, we consider neighboring choices $(3, 4)$ and $(4, 3)$. The systematic uncertainty, σ_{sys} , is estimated as the maximum absolute deviation of these neighboring fits from the central value. The total uncertainty is then computed by adding the statistical and systematic contributions in quadrature:

$$\sigma_{\text{total}} = \sqrt{\sigma_{\text{stat}}^2 + \sigma_{\text{sys}}^2}. \quad (10)$$

4.2 Crossover Temperature T_{pc}^Q and Continuum Estimate

The pseudocritical temperature $T_{pc}^Q(eB)$ at a given magnetic field eB is identified from the peak position of the static quark entropy $S(T, eB)$ obtained using Equation 8. For each bootstrap sample of the entropy surface, the peak temperature is identified. The final reported estimate of $T_{pc}^Q(eB)$ is designated as the median of this distribution, with the 68.27% central quantile as error.

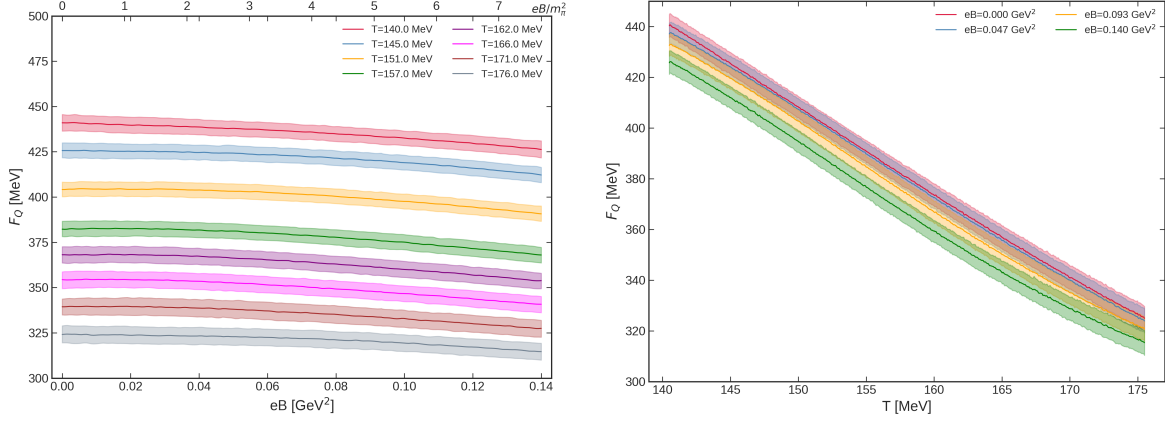


Figure 1: The continuum estimates of F_Q : (left) constant-temperature curves as a function of eB and (right) constant- eB curves as a function of T .

Since the lattice action possesses leading discretization effects of $O(a^2)$, continuum estimates of the observables are obtained using the standard scaling ansatz:

$$O(eB, T, N_\tau) = O(eB, T) + \frac{b}{N_\tau^2}. \quad (11)$$

5. Results

In [Figure 1](#), we show the continuum estimated results for the renormalized static-quark free energy $F_Q(T, eB)$. The left panel shows F_Q as a function of the magnetic field eB for several fixed temperatures. Each curve corresponds to a constant temperature slice of the continuum surface $F_Q(T, eB)$. For all temperatures, the free energy exhibits a mild dependence on eB within the explored weak field range. A slight downward trend with increasing eB is visible for all temperatures, indicating that the free energy associated with inserting a static quark in the system is modestly reduced in the presence of an external magnetic field. The curves are vertically separated according to temperature, suggesting that temperature effects are stronger as compared to eB in affecting a change in F_Q . The smaller temperatures correspond to larger values of F_Q , reflecting reduced color screening characteristic of the confined phase. As temperature increases, F_Q decreases, consistent with enhanced screening at high temperatures.

This effect of weaker screening at lower temperature and low sensitivity to eB is also visible in the right panel of [Figure 1](#) which displays F_Q as a function of temperature for several fixed values of the magnetic field. Each curve represents a constant eB slice of the continuum-interpolated surface. The free energy decreases monotonically with increasing temperature, suggesting enhanced screening of the static color charge in the thermal medium. The inflection point associated with a crossover is difficult to identify by eye, given the limited temperature range analyzed. The separation between curves corresponding to different magnetic fields remains small over the entire temperature range, demonstrating that the magnetic field dependence of F_Q is weak. At fixed temperature, increasing eB mildly lowers the free energy.

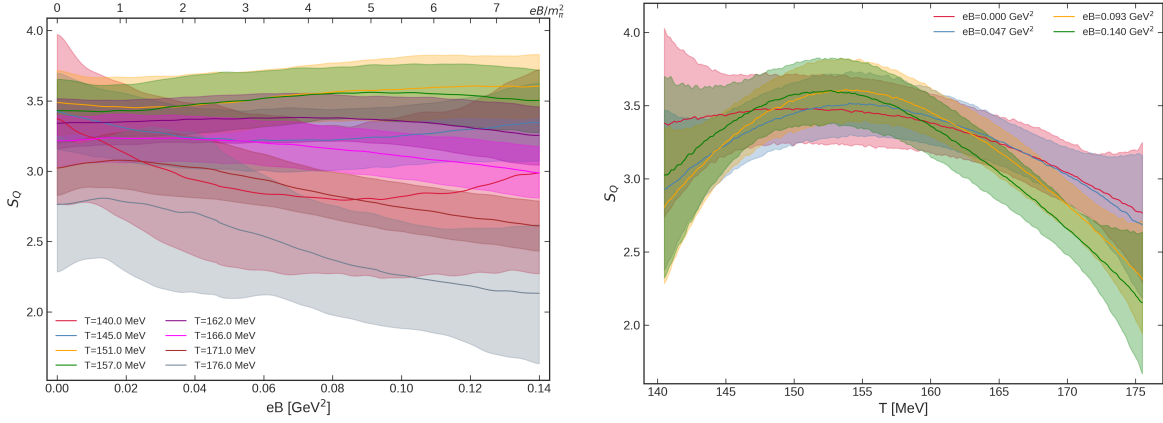


Figure 2: The continuum estimates of S_Q : (left) constant-temperature curves as a function of eB and (right) constant- eB curves as a function of T .

Figure 2 shows the continuum estimates of the static-quark entropy $S_Q(T, eB)$. The left panel shows S_Q as a function of eB for several fixed temperatures. At lower temperatures, S_Q takes smaller values, consistent with a confined medium where the system's response to temperature variations is limited. The slope at these lower temperatures appears mildly positive suggesting a possible decrease in T_{pc}^Q as eB increases. As temperature approaches the crossover region, S_Q is at its maximum. Only a mild variation with eB is observed, indicating mild sensitivity of T_{pc}^Q in the weak-field regime. At higher temperatures, S_Q takes smaller values with negative slope as expected in a deconfined phase.

The right panel of Figure 2 shows S_Q as a function of temperature for several fixed values of eB . For each magnetic field, the entropy exhibits a clear peak structure in the crossover region around $T \sim 153$ MeV. This peak corresponds to the crossover temperature $T_{pc}^Q(eB)$. The peak position shifts only slightly with increasing eB , indicating that the crossover temperature T_{pc}^Q has weak dependence on the magnetic field in the weak-field regime.

Figure 3 (left) shows $T_{pc}^Q(eB)$ as a function of the external magnetic field for lattice temporal extents $N_\tau = 8$ and $N_\tau = 12$, along with their continuum estimate obtained using Equation 11. Lattice estimates at both lattice spacings as well as continuum hold a steady value within error across the eB range explored with a mild downward trend becoming visible in each dataset as eB increases. The continuum estimate is nearly constant at $T_{pc}^Q \approx 153$ MeV. This suggests that the deconfinement indicator defined via the static-quark entropy peak exhibits low sensitivity in the weak field limit.

Figure 3 (right) compares the continuum estimates of $T_{pc}^Q(eB)$ with the corresponding chiral pseudocritical temperature $T_{pc}^X(eB)$ (data obtained from [14]). The two observables coincide within uncertainties for the entire range of eB considered. T_{pc}^X holds a steady value $T_{pc}^X \approx 155$ MeV. While T_{pc}^Q shows a slight decrease with increasing eB , the chiral pseudocritical temperature remains essentially constant throughout the same interval. The T_{pc}^X curve appears nearly horizontal within errors, indicating that chiral symmetry restoration is largely insensitive to magnetic fields up to $eB \approx 0.14$ GeV².

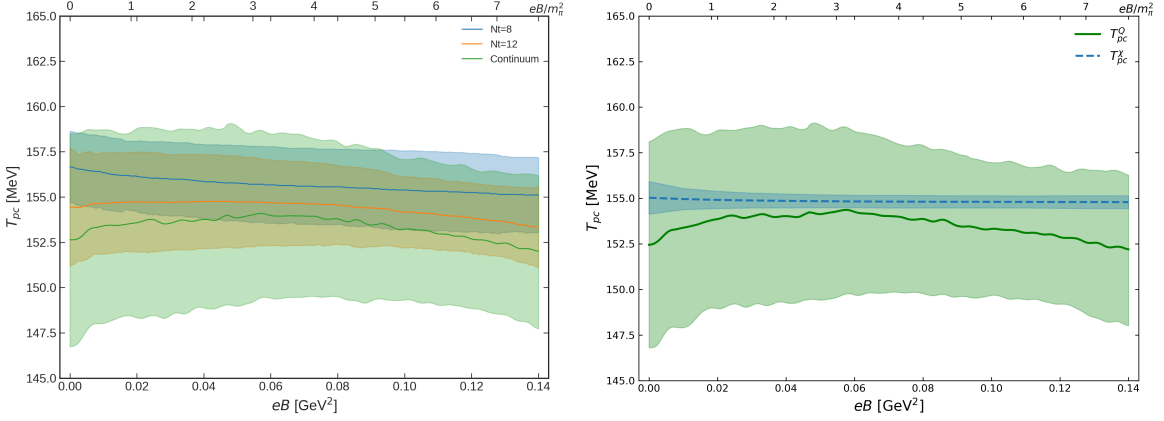


Figure 3: (Left) Continuum estimates of the T_{pc}^Q together with lattice estimates at $N_\tau = 8$ and 12 as functions of the magnetic field eB . (Right) Continuum estimates of T_{pc}^Q and T_{pc}^χ , where T_{pc}^χ is taken from [14], as functions of eB .

6. Conclusion

We presented a continuum estimate of the static-quark free energy and entropy in the presence of external magnetic fields at physical quark masses. The entropy peak, corresponding to the inflection point of the renormalized static-quark free energy, was used as an indicator of the deconfinement-like crossover.

Within the weak field regime explored, $eB \lesssim 0.14 \text{ GeV}^2$, the static-quark entropy peak remains clearly identifiable and exhibits only a mild magnetic field dependence. The associated pseudocritical temperature T_{pc}^Q shows a mild downward trend with increasing eB , but remains approximately constant within current uncertainties, with a continuum estimate around 153 MeV . A direct comparison with the chiral pseudocritical temperature T_{pc}^χ indicates that both observables coincide within errors over the entire magnetic field range considered. This suggests that, in the weak field regime, chiral restoration and deconfinement remain closely correlated phenomena.

This limited magnetic-field sensitivity of T_{pc}^Q contrasts with the enhanced sensitivity to the magnetic field observed in the baryon-electric charge correlator χ_{11}^{BQ} , reflecting changes in the effective degrees of freedom as reported in [14, 15]. It signals that conserved charge fluctuations may probe different aspects of the medium that are more sensitive to magnetic field effects than bulk thermodynamic indicators of screening aspects of the deconfinement phenomenon.

Acknowledgments

This work was supported in part by the National Natural Science Foundation of China under Grants No. 12293064, No. 12293060, and No. 12325508, as well as the National Key Research and Development Program of China under Contract No. 2022YFA1604900 and the Fundamental Research Funds for the Central Universities, Central China Normal University under Grants No. 30101250314 and No. 30106250152, Ministry of Science and Technology of China under Grant No. 2024YFA1611004, NSFC fund under No. 92570117, Shenzhen Peacock fund under No.

2023TC0179. The numerical simulations have been performed on the GPU cluster in the Nuclear Science Computing Center at Central China Normal University (NSC3) and Wuhan Supercomputing Center.

References

- [1] T. Vachaspati, Magnetic fields from cosmological phase transitions, *Phys. Lett. B* 265 (1991) 258–261. doi:10.1016/0370-2693(91)90051-Q.
- [2] R. C. Duncan, C. Thompson, Formation of very strongly magnetized neutron stars - implications for gamma-ray bursts, *Astrophys. J. Lett.* 392 (1992) L9. doi:10.1086/186413.
- [3] D. E. Kharzeev, J. Liao, Chiral magnetic effect reveals the topology of gauge fields in heavy-ion collisions, *Nature Rev. Phys.* 3 (1) (2021) 55–63. arXiv:2102.06623, doi:10.1038/s42254-020-00254-6.
- [4] J. O. Andersen, W. R. Naylor, A. Tranberg, Phase diagram of QCD in a magnetic field: A review, *Rev. Mod. Phys.* 88 (2016) 025001. arXiv:1411.7176, doi:10.1103/RevModPhys.88.025001.
- [5] G. Endrodi, QCD with background electromagnetic fields on the lattice: a review (6 2024). arXiv:2406.19780.
- [6] G. Cao, Recent progresses on QCD phases in a strong magnetic field: views from Nambu–Jona-Lasinio model, *Eur. Phys. J. A* 57 (9) (2021) 264. arXiv:2103.00456, doi:10.1140/epja/s10050-021-00570-0.
- [7] G. S. Bali, F. Bruckmann, G. Endrodi, Z. Fodor, S. D. Katz, A. Schafer, QCD quark condensate in external magnetic fields, *Phys. Rev. D* 86 (2012) 071502. arXiv:1206.4205, doi:10.1103/PhysRevD.86.071502.
- [8] G. S. Bali, F. Bruckmann, G. Endrodi, Z. Fodor, S. D. Katz, S. Krieg, A. Schafer, K. K. Szabo, The QCD phase diagram for external magnetic fields, *JHEP* 02 (2012) 044. arXiv:1111.4956, doi:10.1007/JHEP02(2012)044.
- [9] H. T. Ding, S. T. Li, J. H. Liu, X. D. Wang, Chiral condensates and screening masses of neutral pseudoscalar mesons in thermomagnetic QCD medium, *Phys. Rev. D* 105 (3) (2022) 034514. arXiv:2201.02349, doi:10.1103/PhysRevD.105.034514.
- [10] H.-T. Ding, D. Zhang, Chiral Properties of (2+1)-Flavor QCD in Magnetic Fields at Zero Temperature (1 2026). arXiv:2601.18354.
- [11] M. D’Elia, L. Maio, F. Sanfilippo, A. Stanzione, Confining and chiral properties of QCD in extremely strong magnetic fields, *Phys. Rev. D* 104 (11) (2021) 114512. arXiv:2109.07456, doi:10.1103/PhysRevD.104.114512.

- [12] M. D’Elia, F. Manigrasso, F. Negro, F. Sanfilippo, QCD phase diagram in a magnetic background for different values of the pion mass, *Phys. Rev. D* 98 (5) (2018) 054509. [arXiv:1808.07008](#), [doi:10.1103/PhysRevD.98.054509](#).
- [13] H.-T. Ding, J.-B. Gu, S.-T. Li, R. Thakkar, Chiral condensates and screening masses of neutral pseudoscalar mesons from lattice QCD at physical quark masses, *Phys. Rev. D* 111 (7) (2025) 074513. [arXiv:2501.11262](#), [doi:10.1103/PhysRevD.111.074513](#).
- [14] H.-T. Ding, J.-B. Gu, A. Kumar, S.-T. Li, Second order fluctuations of conserved charges in external magnetic fields, *Phys. Rev. D* 111 (11) (2025) 114522. [arXiv:2503.18467](#), [doi:10.1103/tgm5-jvyf](#).
- [15] H.-T. Ding, J.-B. Gu, A. Kumar, S.-T. Li, J.-H. Liu, Baryon Electric Charge Correlation as a Magnetometer of QCD, *Phys. Rev. Lett.* 132 (20) (2024) 201903. [arXiv:2312.08860](#), [doi:10.1103/PhysRevLett.132.201903](#).
- [16] A. Bazavov, N. Brambilla, H. T. Ding, P. Petreczky, H. P. Schadler, A. Vairo, J. H. Weber, Polyakov loop in 2+1 flavor QCD from low to high temperatures, *Phys. Rev. D* 93 (11) (2016) 114502. [arXiv:1603.06637](#), [doi:10.1103/PhysRevD.93.114502](#).
- [17] A. M. Polyakov, Gauge Fields as Rings of Glue, *Nucl. Phys. B* 164 (1980) 171–188. [doi:10.1016/0550-3213\(80\)90507-6](#).
- [18] O. Kaczmarek, F. Karsch, P. Petreczky, F. Zantow, Heavy quark anti-quark free energy and the renormalized Polyakov loop, *Phys. Lett. B* 543 (2002) 41–47. [arXiv:hep-lat/0207002](#), [doi:10.1016/S0370-2693\(02\)02415-2](#).
- [19] K. Fukushima, Magnetic-field Induced Screening Effect and Collective Excitations, *Phys. Rev. D* 83 (2011) 111501. [arXiv:1103.4430](#), [doi:10.1103/PhysRevD.83.111501](#).
- [20] O. Kaczmarek, F. Zantow, Static quark anti-quark interactions at zero and finite temperature QCD. II. Quark anti-quark internal energy and entropy (6 2005). [arXiv:hep-lat/0506019](#).
- [21] E. Follana, Q. Mason, C. Davies, K. Hornbostel, G. P. Lepage, J. Shigemitsu, H. Trotter, K. Wong, Highly improved staggered quarks on the lattice, with applications to charm physics, *Phys. Rev. D* 75 (2007) 054502. [arXiv:hep-lat/0610092](#), [doi:10.1103/PhysRevD.75.054502](#).
- [22] H. T. Ding, S. T. Li, A. Tomiya, X. D. Wang, Y. Zhang, Chiral properties of (2+1)-flavor QCD in strong magnetic fields at zero temperature, *Phys. Rev. D* 104 (1) (2021) 014505. [arXiv:2008.00493](#), [doi:10.1103/PhysRevD.104.014505](#).
- [23] L. Mazur, et al., SIMULATeQCD: A simple multi-GPU lattice code for QCD calculations, *Comput. Phys. Commun.* 300 (2024) 109164. [arXiv:2306.01098](#), [doi:10.1016/j.cpc.2024.109164](#).
- [24] A. Bazavov, et al., Meson screening masses in (2+1)-flavor QCD, *Phys. Rev. D* 100 (9) (2019) 094510. [arXiv:1908.09552](#), [doi:10.1103/PhysRevD.100.094510](#).